Evaluation of the Tau-Omega Model Over a Dense Corn Canopy at P- and L-Band

Xiaoji Shen, *Member, IEEE*, Jeffrey P. Walker, *Fellow, IEEE*, Nan Ye, Xiaoling Wu, Foad Brakhasi, Liujun Zhu, *Member, IEEE*, Edward Kim, Yann Kerr, *Life Fellow, IEEE*, and Thomas Jackson, *Life Fellow, IEEE*

***Abstract*— As an emerging technique, P-band (0.3–1 GHz) may improve soil moisture remote sensing compared to L-band (1.4 GHz) Soil Moisture and Ocean Salinity (SMOS) and Soil Moisture Active Passive (SMAP) missions, because of its greater moisture retrieval depth resulting from its longer wavelength. Consequently, a number of tower-based experiments were undertaken in VIC, Australia, to understand and quantify potential improvements. The study reported here has extended the evaluation of the tau-omega model to a scenario with a dense corn canopy whose vegetation water content (VWC) reached ∼20 kg/m^2, and compared the soil moisture retrieval performance at P- and L-band. Based on the locally calibrated parameters, the results from both the single-channel algorithm (SCA) and dual-channel algorithm (DCA) approaches presented a clear reduction in vegetation impact at the P-band compared to L-band. While the root-mean-square error (RMSE) for the P-band did not achieve the 0.04-m^3/m^3 target accuracy of SMOS and SMAP, i.e., 0.054 m^3/m^3 for the SCA and 0.074 m^3/m^3 for the DCA, this performance can be regarded as acceptable considering the extremely high VWC. In comparison, the RMSEs at L-band were larger than 0.1 m^3/m^3 for both the SCA and the DCA approaches. Additionally, DCA performed better in correlation coefficient and unbiased RMSE, while SCA performed better in RMSE at the P-band due to the larger bias when using DCA. Moreover, the calibrated vegetation parameters at the P-band were found to apply to broader conditions than those at the L-band, likely due to the reduced vegetation impact.**

***Index Terms*— P-band, passive microwave, roughness, soil moisture retrieval, vegetation.**

Manuscript received 1 October 2022; revised 8 December 2022, 24 February 2023, and 17 April 2023; accepted 4 May 2023. Date of publication 15 September 2023; date of current version 5 October 2023. This work was supported in part by the National Natural Science Foundation of China under Grant 52309017 and Grant 42371369, in part by the Natural Science Foundation of Jiangsu Province under Grant BK20230958 and Grant BK20210377, and in part by the Australian Research Council under Grant DP170102373. *(Corresponding author: Xiaoji Shen.)*

Xiaoji Shen and Liujun Zhu are with the Yangtze Institute for Conservation and Development, Hohai University, Nanjing 210024, China, and also with the Department of Civil Engineering, Monash University, Clayton, VIC 3800, Australia (e-mail: xiaoji.shen@hhu.edu.cn).

Jeffrey P. Walker, Nan Ye, Xiaoling Wu, and Foad Brakhasi are with the Department of Civil Engineering, Monash University, Clayton, VIC 3800, Australia.

Edward Kim is with the NASA Goddard Space Flight Center, Greenbelt, MD 20771 USA.

Yann Kerr is with the Centre d'Etudes Spatiales de la Biosphère, 31401 Toulouse, France.

Thomas Jackson, retired, was with the USDA ARS Hydrology and Remote Sensing Laboratory, Beltsville, MD 20705 USA. He resides in Valencia, CA 91354 USA.

Digital Object Identifier 10.1109/LGRS.2023.3315869

I. Introduction

SOIL moisture is an essential indicator of climate change, controlling various processes in the water, energy, and carbon exchanges between the atmosphere and the land surface [1]. There are two L-band (∼21-cm wavelength/1.4 GHz) satellite missions currently operating for observing global soil moisture: the Soil Moisture and Ocean Salinity (SMOS) mission of the European Space Agency [2] and the Soil Moisture Active Passive (SMAP) mission of the National Aeronautics and Space Administration [3]. These state-of-the-art missions make it possible to map global near-surface soil moisture four times every three days or less, with a target accuracy of 0.04 m^3/m^3. However, these measurements are limited to a relatively shallow moisture retrieval depth, which is commonly held to be within the top 5 cm at L-band. Moreover, the soil moisture retrieval at L-band is degraded by the soil surface roughness and vegetation canopy. However, radiative transfer theory predicts that longer wavelength observations, such as at P-band (100–30-cm wavelength/0.3–1.0 GHz), provide information on a deeper depth of soil and a potentially improved estimation accuracy as a result of the reduced impact of surface roughness. Recently, the P-band Radiometer Inferred Soil Moisture (PRISM, see https://www.prism.monash.edu) tower project of Monash University, Clayton, VIC, Australia, has experimentally verified this expectation [4], [5], [6].

The vegetation canopy is well-known for reducing the brightness temperature (TB) sensitivity to soil moisture by adding its contribution to the total emission and attenuating the soil emission [7]. Consequently, the vegetation attenuation becomes more substantial as the vegetation water content (VWC) increases. It has been identified that the radiometric sensitivity to soil moisture at 1.4 GHz at the nadir was 3.1 K per 0.01 m^3/m^3 for bare soil and 1.1 K per 0.01 m^3/m^3 for a corn canopy with 5-kg/m^2 VWC [8]. However, when the VWC increased to 6.3 kg/m^2 for corn, the radiometric sensitivity to soil moisture reduced to 1.0 K per 0.01 m^3/m^3 at 1.4 GHz and V-polarization [9]. Moreover, the difference in vegetation structure (i.e., the distribution of the dielectric constant) can also contribute to the opacity of the vegetation canopy; Wang et al. [10] observed no radiometric sensitivity to soil moisture through a grass canopy with a biomass density of 8 kg/m^2 at 1.4 GHz, whereas for a corn canopy with the same biomass density, it was 1.0 K per 0.01 m^3/m^3 at V-polarization [9].

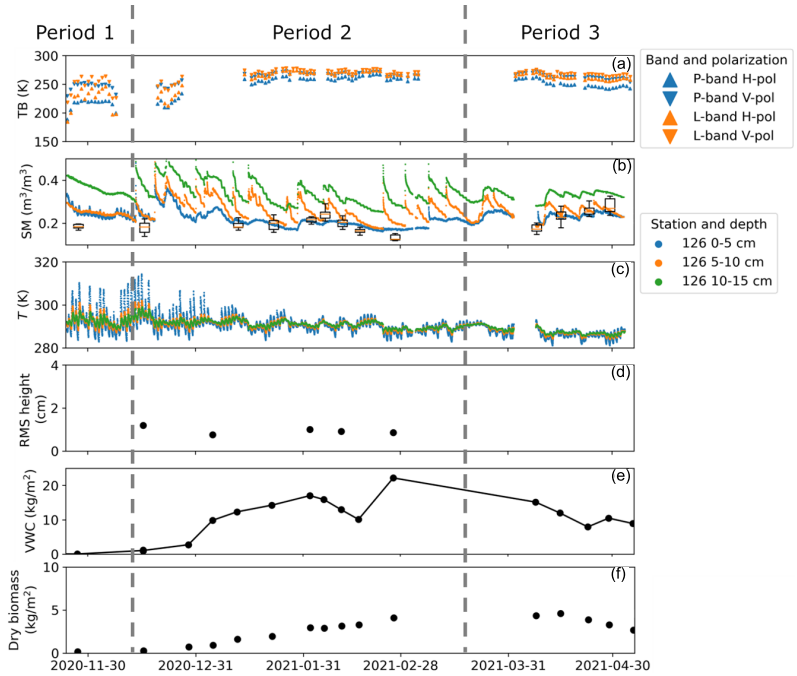

Fig. 1. Data collected over the corn-growing cycle, including: (a) TB observations at 6 A.M., with the data gaps caused by the tower lowering due to high wind in December 2020 and January 2021 and by the instrument removal due to the airborne experiment in March 2021; (b) station soil moisture together with HDAS observations (boxplots); (c) station soil temperature; (d) rms height averaged from the roughness measurements in two perpendicular directions; (e) observed (dots) with linearly interpolated (line) VWC; and (f) observed dry biomass. For clarity, only the data measured from the top three probes are plotted in (b) and (c).

Mo et al. [11] proposed the tau-omega ($\tau - \omega$) model to relate the TB of vegetation-covered soil to its moisture content, where τ and ω are optical depth and single scattering albedo, respectively. Based upon this model, the single-channel algorithm (SCA) [12] and the dual-channel algorithm (DCA) [13] have been developed for SMAP.

Shen et al. [4] undertook the first evaluation of the τ–ω model at P-band. They identified that for low-to-intermediate vegetation, i.e., wheat with under 4-kg/m^2 VWC, the use of the P-band achieved a similar retrieval performance to the L-band when using the SCA-V approach with the τ–ω model. This motivated an investigation of corn in this letter, which has a similar vertical structure but a much higher VWC. This investigation managed to plant corn with an approximately 12-m^{-2} plant density resulting in the VWC peaking at 21.05 kg/m^2. Accordingly, the retrieval performance at P- and L-band was evaluated and compared successively using the SMAP SCA-V and DCA τ–ω approaches under a high VWC.

II. Data

The PRISM tower site was established at Cora Lynn, VIC, from October 2017 to May 2021. A ten-meter-high tower was set up in the field, hosting two dual linear [horizontal (H) and vertical (V)] radiometers, namely, the Polarimetric L-band Multibeam Radiometer (PLMR) at 1.401–1.425 GHz and the Polarimetric P-band Multibeam Radiometer (PPMR) at 0.742–0.752 GHz.

The study period in this letter is the corn-growing cycle from November 24, 2020, to May 4, 2021, when the field was managed with a flat surface condition. The corn was planted very densely with approximately 12 plants per square meter to achieve a high VWC, with a 45° angle between the row direction and the tower look direction. A station measured the soil moisture and soil temperature variation above the 60-cm layer at 5-cm intervals. Additionally, the hydra-probe data acquisition system (HDAS) was used to detect the spatial variation in 5-cm soil moisture across the field [shown in the boxplots in Fig. 1(b)]. The agreement between HDAS measurements and the station soil moisture confirmed the representativeness of the station.

The P-band TB data at 40° and the L-band TB data at 38° incidence angle [Fig. 1(a)] were used in this letter. The ~1-cm root-mean-square height (rms height) measurements confirmed that the soil was electromagnetically flat [Fig. 1(d)]. The soil was a silt loam with 0.87-kg/m^3 bulk density, 18.0% clay, 10.9% sand, and 71.1% silt. Please also refer to the preceding studies [4], [5], [6] for more comprehensive descriptions of the PRISM tower experiment.

The dataset used herein was divided into three segments (Fig. 1): 1) the bare soil period from November 24 to December 9, 2020, being before the corn emergence; 2) from December 18, 2020, to March 7, 2021, being after the corn emergence; and 3) from April 1 to May 4, 2021, when the water content of corn was decreasing. The VWC and dry biomass measurements estimated from destructive vegetation samples are plotted in Fig. 1(e) and (f), respectively. Frequent irrigation was conducted over the field to meet the corn's high water demands. The declined VWC in early February was possibly attributed to paused irrigation and high air temperature. After restarting irrigation on February 23, the VWC rocketed to 21.05 kg/m^2.

III. Method

Please refer to [4] for a full description of the forward modeling. The τ–ω model [11] characterizes the thermal

microwave emission (TB_p, where subscript p denotes polarizations) from a vegetation-covered surface, formulated as

$$TB_p = (1-\omega)(1-\gamma_p)T_{eff}^{v} + (1-\omega)(1-\gamma_p)\gamma_p\Gamma_p T_{eff}^{v} + (1-\Gamma_p)\gamma_p T_{eff}^{s} + TB^{sky\_down}\Gamma_p\gamma_p^2 \quad (1)$$

where T_{eff}^{v} and γ_p are the vegetation canopy's effective temperature and transmissivity, respectively, and T_{eff}^{s} and Γ_p are the soil's effective temperature and reflectivity, respectively. The TB^{sky_down} was taken to be 5.3 K at the L-band and 13.9 K at the P-band [14]. The HQN model was used to estimate Γ_p [15], such that

$$\Gamma_p = \left[(1-Q_R)\Gamma_p^* + Q_R\Gamma_q^*\right]\exp\left[-H_{Rp}\cos^{N_{Rp}}(\theta)\right] \quad (2)$$

where Γ_p^* is the specular reflectivity calculated from the Fresnel equations. The roughness parameters H_{Rp}, Q_R, and N_{Rp} were assumed to be constant during the study period because the surface roughness was found to have little change according to Fig. 1(d).

The dielectric model by Mironov et al. [16] was used in this investigation because it considers the interfacial relaxation of soil water at P-band. The effective soil temperature was calculated using the physical model by Choudhury et al. [17], which does not contain any empirical parameter to be determined. As in [4], the averaged soil moisture data collected at roughly 6 A.M. in the 0–5-cm soil layer from the station [Fig. 1(b)] were utilized for simulating TB and evaluating the retrieval results in this letter.

The SMAP SCA-V and DCA approaches were successively implemented, with the cost functions described in [4]. For the SCA-V approach, τ was estimated by multiplying the VWC by parameter b [18], and $Q_R = 0$ and $N_{RV} = 2$ were assumed based on the SMAP SCA baseline algorithm. A three-step SCA-V approach was employed: 1) the H_R parameter was calibrated using the data collected over period 1; 2) based on the H_R from 1), the b and ω parameters were calibrated using the V-pol TB, soil moisture, soil temperature, and VWC observations collected in period 3; and 3) soil moisture was retrieved using the calibrated parameters from the first two steps and the V-pol TB observations collected in period 2. Note that assuming constant parameters through different vegetative stages may bring uncertainties [19].

In terms of the DCA, it was assumed that $N_{Rp} = 2$ and $\omega = 0.06$ for croplands as in the SMAP DCA implementation [20]. A two-step DCA approach was employed: 1) calibrate H_R and Q_R using the data collected over period 1 and 2) retrieve soil moisture and τ using the H_R and Q_R from 1) and the dual-pol TB observations from periods 2 and 3.

IV. Results

Use of the SMAP SCA default parameters for croplands ($H_R = 0.108$, $Q_R = 0$, $N_R = 2$, $b = 0.11$, and $\omega = 0.05$) was first evaluated at V-pol TB over periods 2 and 3 (result not shown), with unacceptable retrieval performance at both P- and L-band, i.e., ~0.5-m^3/m^3 root-mean-square error (RMSE). Therefore, the model parameters (H_R, b, and ω) needed to be calibrated at this site.

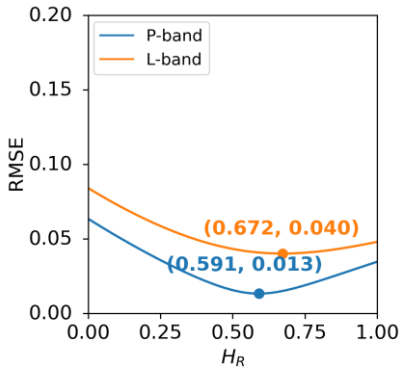

Fig. 2. RMSE between the simulated and observed emissivity at V-pol over period 1 using different values of H_R. The dots with values show the minimal RMSE and the corresponding H_R values. The values of Q_R and N_{RV} were assumed to be 0 and 2, respectively, at both P- and L-band.

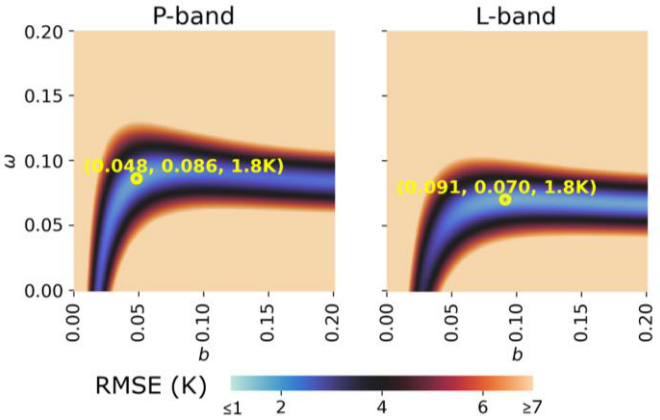

Fig. 3. RMSE (K) between the simulated and observed TB at V-pol over period 3 using different values of b and ω. The yellow circles represent where the minimal RMSE was obtained, with the three values indicating b, ω, and the minimum RMSE, respectively. The values of H_R calibrated from period 1 were used, namely, 0.591 for P-band and 0.672 for L-band. The values of Q_R and N_{RV} were assumed to be 0 and 2, respectively, at both P- and L-band.

The first step of the SCA-V approach was performed to calibrate H_R using the data collected over period 1. The V-pol emissivity was simulated using a number of H_R values for the bare soil in period 1. The optimal H_R values are marked as the dots in Fig. 2, which yielded the lowest RMSE between the observed and simulated emissivity. Therefore, H_R was calibrated to be 0.591 and 0.672 at the P- and L-band, respectively, with the calibration residuals being 0.04 at the P-band and 0.013 at the L-band.

The second step of the SCA-V approach was performed to calibrate b and ω using the data collected over period 3. In Fig. 3, the soil moisture measurements collected over period 3 were used to simulate TB with calibrated H_R (Fig. 2) and varying b and ω. As a result, b and ω were calibrated to be 0.048 and 0.086 for P-band and 0.091 and 0.070 for L-band. The calibration residual was 1.8 K at both P- and L-band. Gao et al. [21] found that the b values increased with increasing frequency, which was confirmed at P- and L-band in Fig. 3. Microwave radiometry theory predicts that ω reduces as frequency decreases since a longer wavelength band is expected to have minor scattering effects. However, the higher ω at P- than L-band calibrated in Fig. 3 is contrary to the theory, as also reported in [8] and [11], potentially because

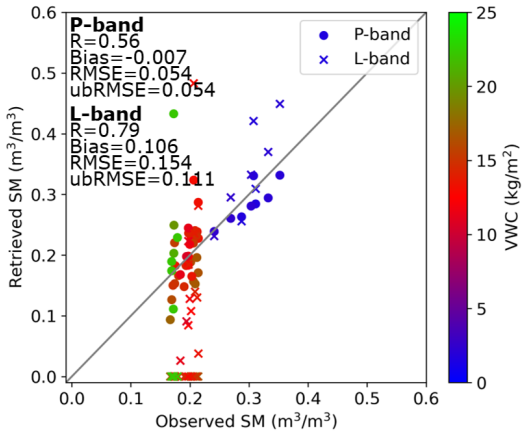

Fig. 4. Observed versus retrieved soil moisture for period 2 of the corn-covered soil, using the SCA-V with the τ–ω model [see (1)]. The color indicates the VWC for each soil moisture measurement. The calibrated H_{R}, b, and ω parameters were used here, i.e., $H_{\mathrm{R}} = 0.591$, $b = 0.048$, and $\omega = 0.086$ for P-band and $H_{\mathrm{R}} = 0.672$, $b = 0.091$, and $\omega = 0.070$ for L-band. The default SMAP SCA Q_{R} (=0) and N_{RV} (=2) were used for both P- and L-band.

ω became an effective parameter that is sensitive to higher order scattering.

The third step of the SCA-V approach was performed to retrieve soil moisture, with the results plotted against observations in Fig. 4. For VWC lower than 5 kg/m^2, the scatter points at L-band deviated further from the 1:1 line than those at P-band (Fig. 4). When the VWC was higher than 10 kg/m^2, the retrieved soil moisture at P-band reasonably ranged from 0.1 to 0.25 m^3/m^3, while zero values were retrieved at L-band. The RMSEs at P- and L-band were 0.054 and 0.154 m^3/m^3, respectively; while the RMSE/ubRMSE did not achieve the 0.04-m^3/m^3 target accuracy of SMAP and SMOS, the performance at P-band was acceptable considering the high VWC of up to $\sim$20 kg/m^2.

Although the correlation coefficient at the L-band (0.79) was higher than that at the P-band (0.56), it was reduced to 0.62 after excluding the zero values in calculating the statistics at the L-band. The RMSE at the L-band was also reduced to 0.101 m^3/m^3 after excluding the zero values, being still substantially larger than that for the P-band. The zero values of L-band retrieval in Fig. 4 are likely due to different VWCs for the calibration and validation datasets, being up to $\sim$15 and $\sim$20 kg/m^2, respectively, and therefore, the calibrated vegetation parameters might have incorrectly constrained the calculation of the vegetation variables, e.g., τ and ω. Additionally, multiple scattering and/or the assumed static ω could have led to the poor performance at the L-band.

When applying the calibrated vegetation parameters to the validation dataset at the L-band, the modeled TB was lower than the observed TB, even though the soil moisture was zero at the beginning of the retrieval iteration. Therefore, the soil moisture was bound to be zero since an increase in soil moisture further decreases the modeled TB and thus enlarges the cost function. This phenomenon indicated that at L-band the calibrated parameters may not be transferred to applications with vegetation conditions substantially different from the calibration dataset. Conversely, the calibrated vegetation parameters at P-band were found to apply to a broad range of conditions, likely due to the reduced vegetation impact.

TABLE I
CALIBRATED DCA ROUGHNESS PARAMETERS USING THE DATA FOR PERIOD 1

Band	H_R	Q_R
P	0.683	0.066
L	0.789	0.096

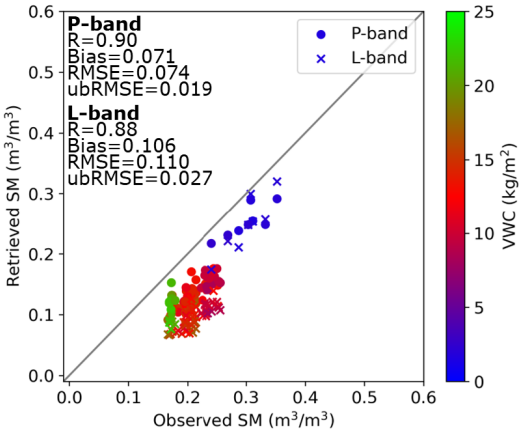

Fig. 5. Observed versus retrieved soil moisture for periods 2 and 3 of the corn-covered soil, using the DCA approach. The color indicates the VWC for each soil moisture measurement. The default values of N_{Rp} and ω in the SMAP DCA algorithm were applied, namely, $N_{\mathrm{Rp}} = 2$ and $\omega = 0.06$, for both P- and L-band. The values of H_{R} and Q_{R} that were calibrated from period 1 (Table I) were used herein.

According to the prior study on wheat with under 4-kg/m^2 VWC [4], the RMSE achieved 0.029 m^3/m^3 for P-band and 0.063 m^3/m^3 for L-band V-pol when completely ignoring the vegetation existence. After calibrating and applying the τ–ω model, the RMSE at P- and L-band reached 0.009 and 0.018 m^3/m^3 for the SCA-V approach. This current investigation over corn-covered soil confirmed that the difference between the RMSEs for PPMR and PLMR became more substantial when the vegetation was much denser.

The first step of the DCA approach was performed to calibrate H_{R} and Q_{R} using the data collected in period 1, with the results shown in Table I. Subsequently, the DCA soil moisture retrieval was conducted using the calibrated H_{R} and Q_{R} in Table I, with the comparison of the retrieved and observed soil moisture plotted in Fig. 5. P-band was found to have a similar R (0.90) as L-band (0.88), while a better RMSE was found at P-band (0.074 m^3/m^3) than L-band (0.110 m^3/m^3). In addition, the retrieved soil moisture for P- and L-band underestimated observed soil moisture, with biases being 0.071 m^3/m^3 at P-band and 0.106 m^3/m^3 at L-band. When the VWC was lower than 5 kg/m^2, the P- and L-band scatter points seemed similar. However, when the VWC was higher than 10 kg/m^2, the scatter points at L-band deviated further from the 1:1 line than those at P-band, with RMSEs being 0.074 m^3/m^3 at P-band and 0.112 m^3/m^3 at L-band. The retrieval error could be reduced if ω is locally calibrated in future studies.

V. Conclusion

In this letter, P- and L-band soil moisture retrieval was performed using the τ–ω model and the SCA-V and DCA approaches. L-band was found to have RMSEs higher than 0.1 m^3/m^3 for both approaches, while the RMSEs at P-band were 0.054 m^3/m^3 for the SCA and 0.074 m^3/m^3 for the DCA, which might be considered acceptable in such extremely high VWC conditions. Accordingly, this letter lends confidence to the use of even lower frequency (e.g., below 0.5 MHz) observations for sensing more accurate soil moisture. Moreover, DCA performed better in correlation coefficient and unbiased RMSE, while SCA performed better in RMSE at the P-band due to the larger bias when using DCA.

Acknowledgment

Gratitude is given to Pascal Mater and Kiri Mason for their assistance with maintaining the experimental equipment and site. The authors also wish to thank Wayne Tymensen for kindly providing the land for the experimental site.

References

[1] S. I. Seneviratne et al., "Investigating soil moisture–climate interactions in a changing climate: A review," *Earth-Sci. Rev.*, vol. 99, nos. 3–4, pp. 125–161, May 2010, doi: 10.1016/j.earscirev.2010.02.004.

[2] Y. H. Kerr et al., "The SMOS mission: New tool for monitoring key elements of the global water cycle," *Proc. IEEE*, vol. 98, no. 5, pp. 666–687, May 2010, doi: 10.1109/JPROC.2010.2043032.

[3] D. Entekhabi et al., "The soil moisture active passive (SMAP) mission," *Proc. IEEE*, vol. 98, no. 5, pp. 704–716, May 2010, doi: 10.1109/JPROC.2010.2043918.

[4] X. Shen et al., "Evaluation of the tau-omega model over bare and wheat-covered flat and periodic soil surfaces at P- and L-band," *Remote Sens. Environ.*, vol. 273, May 2022, Art. no. 112960.

[5] X. Shen et al., "Impact of random and periodic surface roughness on P- and L-band radiometry," *Remote Sens. Environ.*, vol. 269, Feb. 2022, Art. no. 112825, doi: 10.1016/j.rse.2021.112825.

[6] X. Shen et al., "Soil moisture retrieval depth of P- and L-band radiometry: Predictions and observations," *IEEE Trans. Geosci. Remote Sens.*, vol. 59, no. 8, pp. 6814–6822, Aug. 2021, doi: 10.1109/TGRS.2020.3026384.

[7] T. J. Jackson, T. J. Schmugge, and J. R. Wang, "Passive microwave sensing of soil moisture under vegetation canopies," *Water Resour. Res.*, vol. 18, no. 4, pp. 1137–1142, Aug. 1982, doi: 10.1029/WR018i004p01137.

[8] F. T. Ulaby, M. Razani, and M. C. Dobson, "Effects of vegetation cover on the microwave radiometric sensitivity to soil moisture," *IEEE Trans. Geosci. Remote Sens.*, vol. GRS-21, no. 1, pp. 51–61, Jan. 1983.

[9] B. K. Hornbuckle and A. W. England, "Radiometric sensitivity to soil moisture at 1.4 GHz through a corn crop at maximum biomass," *Water Resour. Res.*, vol. 40, p. W10204, Oct. 2004.

[10] J. R. Wang, J. C. Shiue, S. L. Chuang, R. T. Shin, and M. Dombrowski, "Thermal microwave emission from vegetated fields: A comparison between theory and experiment," *IEEE Trans. Geosci. Remote Sens.*, vol. GRS-22, no. 2, pp. 143–150, Mar. 1984.

[11] T. Mo, B. J. Choudhury, T. J. Schmugge, J. R. Wang, and T. J. Jackson, "A model for microwave emission from vegetation-Covered fields," *J. Geophys. Res., Oceans*, vol. 87, no. 13, pp. 11229–11237, Dec. 1982.

[12] T. J. Jackson, "III. Measuring surface soil moisture using passive microwave remote sensing," *Hydrolog. Processes*, vol. 7, no. 2, pp. 139–152, Apr. 1993.

[13] E. G. Njoku, T. J. Jackson, V. Lakshmi, T. K. Chan, and S. V. Nghiem, "Soil moisture retrieval from AMSR-E," *IEEE Trans. Geosci. Remote Sens.*, vol. 41, no. 2, pp. 215–229, Feb. 2003, doi: 10.1109/TGRS.2002.808243.

[14] *International Telecommunication Union Recommendation: Radio Noise*, document ITU-R P.372-12, 2015. [Online]. Available: https://www.itu.int/rec/R-REC-P.372-12-201507-S/en

[15] B. J. Choudhury, T. J. Schmugge, A. Chang, and R. W. Newton, "Effect of surface roughness on the microwave emission from soils," *J. Geophys. Res., Oceans*, vol. 84, no. 9, pp. 5699–5706, Sep. 1979, doi: 10.1029/JC084iC09p05699.

[16] V. L. Mironov, P. P. Bobrov, and S. V. Fomin, "Multirelaxation generalized refractive mixing dielectric model of moist soils," *IEEE Geosci. Remote Sens. Lett.*, vol. 10, no. 3, pp. 603–606, May 2013.

[17] B. J. Choudhury, T. J. Schmugge, and T. Mo, "A parameterization of effective soil temperature for microwave emission," *J. Geophys. Res. Oceans*, vol. 87, no. 2, pp. 1301–1304, Feb. 1982.

[18] T. J. Jackson and T. J. Schmugge, "Vegetation effects on the microwave emission of soils," *Remote Sens. Environ.*, vol. 36, no. 3, pp. 203–212, Jun. 1991.

[19] B. K. Hornbuckle, A. W. England, R. D. De Roo, M. A. Fischman, and D. L. Boprie, "Vegetation canopy anisotropy at 1.4 GHz," *IEEE Trans. Geosci. Remote Sens.*, vol. 41, no. 10, pp. 2211–2223, Oct. 2003.

[20] P. O'Neill et al. (2021). *SMAP Algorithm Theoretical Basis Document (ATBD) Level 2 & 3 Soil Moisture (passive) Data Products Revision G*. Jet Propuls. Lab. [Online]. Available: https://nsidc.org/data/smap/technical-references

[21] Y. Gao et al., "Multi-frequency radiometer-based soil moisture retrieval algorithm parametrization using in situ validation sites," in *Proc. IEEE Int. Geosci. Remote Sens. Symp. (IGARSS)*, Jul. 2017, pp. 3945–3948.